BMC Oral Health

RESEARCH

Open Access

Improved new bone formation capacity of hyaluronic acid-bone substitute compound in rat calvarial critical size defect

Ningbo Zhao[1,2], Lei Qin[3], Yi Liu[4], Min Zhai[5] and Dehua Li[4*]

Abstract

Background Bone loss of residual alveolar ridges is a great challenge in the field of dental implantology. Deproteinized bovine bone mineral (DBBM) is commonly used for bone regeneration, however, it is loose and difficult to handle in clinical practice. Hyaluronic acid (HA) shows viscoelasticity, permeability and excellent biocompatibility. The aim of this study is to evaluate whether high-molecular-weight (MW) HA combined with DBBM could promote new bone formation in rat calvarial critical size defects (CSDs).

Materials and methods Rat calvarial CSDs (5 mm in diameter) were created. Rats ($n=45$) were randomly divided into 3 groups: HA-DBBM compound grafting group, DBBM particles only grafting group and no graft group. Defect healing was assessed by hematoxylin-eosin staining and histomorphometry 2, 4 and 8 weeks postop, followed by Micro-CT scanning 8 weeks postop. Statistical analyses were performed by ANOVA followed by Tukey's post hoc test with $P<0.05$ indicating statistical significance.

Results All rats survived after surgery. Histomorphometric evaluation revealed that at 2, 4 and 8 weeks postop, the percentage of newly formed bone was significantly greater in HA-DBBM compound grafting group than in the other two groups. Consistently, Micro-CT assessment revealed significantly more trabecular bone (BV/TV and Tb.N) in HA-DBBM compound group than in the other two groups, respectively ($P<0.05$). Moreover, the trabecular bone was significantly more continuous (Tb.Pf) in HA-DBBM compound group than in the other two groups, respectively ($P<0.05$).

Conclusion HA not only significantly promoted new bone formation in rats calvarial CSDs but also improved the handling ability of DBBM.

Keywords Hyaluronic acid, Bone substitute, Critical size defect, Bone formation, Handling ability

*Correspondence:
Dehua Li
lidehua@fmmu.edu.cn
[1] Key Laboratory of Shaanxi Province for Craniofacial Precision Medicine Research, College of Stomatology, Xi'an Jiaotong University, 98 XiWu Road, Xi'an, Shaanxi 710004, People's Republic of China
[2] Department of Implant Dentistry, College of Stomatology, Xi'an Jiaotong University, 98 XiWu Road, Xi'an, Shaanxi 710004, People's Republic of China
[3] DeLun Dental, Baiyun District, Guangzhou, Guangdong Province 510080, People's Republic of China
[4] State Key Laboratory of Military Stomatology, Department of Oral Implants, School of Stomatology, Fourth Military Medical University, No. 145 Changle West Road, Xi'an, Shaanxi 710032, People's Republic of China
[5] Department of Stomatology, General Hospital of the Tibet Military Area Command, Lhasa, Tibet 850007, People's Republic of China

Introduction

Currently, titanium dental implants are widely recognized for their efficacy and reliability in addressing both partial and complete tooth loss [1–5]. However, the dental implant field is confronted with the significant challenge of bone loss, which can stem from periodontal disease, trauma, anatomical constraints, congenital issues, or the ongoing resorption of residual alveolar ridges [6–8]. Adequate amount of bone tissue (both width and height) is a prerequisite for the successful placement of implants in the ideal prosthetic-driven position in order to provide a functional and aesthetic implant-retained restoration for patients. Guided bone regeneration (GBR) is the main solution to the problem of bone deficiency at the recipient site. A variety of bone grafting materials are employed in GBR procedures, including autograft, allograft, xenograft, and tissue-engineered bone, each with its own set of benefits and limitations [9].

Deproteinized bovine bone mineral (DBBM) has emerged as a prevalent bone substitute material in GBR. As a osteoconductive scaffold for bone formation, it is widely used in peri-implant bone defects, sinus floor elevation, alveolar ridge augmentation, bone defects between implant and adjacent tooth, and bone loss resulting from periodontal disease [10–14]. To stimulate bone formation, it is recommended that DBBM can be used in combination with autologous bone [15, 16]. However, the availability of bone volume for grafting is inherently limited, and the potential morbidity associated with the donor site must be carefully weighed [17, 18]. Another approach is to add growth factors to bone substitute particles [19, 20], yet issues regarding the high cost and the biosafety of growth factors need to be properly addressed. Furthermore, bone substitute particles is loose, and can be washed away by blood or flushing fluid in clinical practice [21, 22]. It lacks cohesion and can't maintain the space where it is grafted, while space maintenance is one of the four key biological factors (known as PASS principle) for predictable bone regeneration in GBR [23]. Consequently, improving the handling ability of bone substitute particles while preserving bone graft effectiveness is an urgent problem to be solved.

Hyaluronic acid (HA), which exists in various tissues of mammals, is a commonly used hydrogel [24]. As a principal constituent of the extracellular matrix, HA exhibits viscoelasticity, permeability, and excellent biocompatibility. It participates in several critical biological processes, such as cellular signaling [25], cell adhesion and proliferation, cell differentiation [26–31], chondrogenesis [32], osteogenesis [33], anti-inflammatory [34] and pro-angiogenesis [35]. Hydrogel, as excipient, combined with bone substitute might provide a feasible solution to the challenges faced in bone grafting. The viscoelasticity of HA is correlated with its molecular weight (MW). The higher the MW of HA, the greater the viscoelasticity of HA becomes.

Moreover, it has been proven in some studies that high-MW HA had bacteriostatic effect, inhibiting the growth of several bacteria, such as Sreptococcus, Porphyromonas gingivals, and Actinobacillus [36]. Our previous study have showed that HA with higher MW and concentration promoted bone formation in vitro [37]. Additionally, Asparuhova et al. [31] reported that HA induces the growth of mesenchymal stromal cells and pre-osteoblasts and maintains their stemness in vitro. Because of its osteoinductive, bacteriostatic, and anti-inflammatory properties, HA was proven to improve bone formation and accelerate wound healing in extraction sockets with chronic pathology in dogs [38]. These studies speak in favor of the clinical potential of high-MW HA in bone regeneration.

Based upon these studies, it is necessary to evaluate the new bone formation capacity of high-MW HA combined with DBBM. Therefore, we established the rat calvarial critical size defects (CSDs) model and assessed the new bone formation capacity of the HA-DBBM compound, trying to provide some information for understanding the mechanism of the new bone formation, and provide scientific evidence for further optimizing the properties of bone substitute particles. The null hypothesis was that high-MW HA combined with DBBM could not promote new bone formation.

Materials and methods

Experimental animals

Forty-five male Sprague–Dawley (SD) rats aged 7 to 8 weeks and weighing 290 to 320 g, were purchased from the Experimental Animal Center of the Fourth Military Medical University. Before use, the rats were housed under 12 h light/dark cycle (at the room temperature of 24 ± 1℃ and humidity of 60 ± 10%) for 1 week. The bedding, food and water were all sterilized. All the experimental procedures were approved by the Laboratory Animal Care & Welfare Committee, School of Stomatology, Fourth Military Medical University. SD rats were randomly divided into 3 groups, HA-DBBM compound grafting group, DBBM particles only grafting group and no graft group (the test group, the negative control group and the blank control group, respectively).

Preparation of HA solution and HA-DBBM compound

HA with the MW of 2630 kDa was purchased from Bloomage Freda Biopharm Co., Ltd., Shandong, China. It was dissolved in phosphate buffered saline to prepare an HA solution with the concentration of 2 mg/mL. DBBM particles (Geistlich Pharma AG, Wolhusen, Switzerland)

(900 mg) were added to 1 mL HA solution and mixed to prepared HA-DBBM compound.

Surgical procedures

Surgical procedures were performed under sterile conditions. SD rats were generally anesthetized via an intraperitoneal injection of 1% sodium pentobarbital (0.30 mL/100 g). The surgical site was disinfected with povidone iodine (Fig. 1A). An approximately 15 to 20 mm long sagittal incision was made. The skin and periosteum of the rat calvarium were carefully elevated and reflected (Fig. 1B). Two symmetrical round full-thickness calvarial CSDs (5 mm in diameter) were created using a trephine drill (No. 22349.04, Stoma, Germany), one in each parietal bone (Fig. 1C). Constant irrigation with sterile sodium chloride was applied to prevent overheating of the bone tissue. Both defects in each rat were filled with the same materials or no graft (Fig. 1D-F). The bioresorbable collagen membrane Bio-Gide® (Geistlich Pharma AG, Wolhusen, Switzerland) was used to cover the bone defects (Fig. 1G). After that, the periosteum and skin were sutured in layers with absorbable and 4–0 silk sutures, respectively (Fig. 1H-I). Cefazolin sodium was subcutaneously injected to prevent wound infection 1 to 7 days postop.

Clinical observation of rat calvarial CSDs

Nine rats were sacrificed by overdose injection of 1% sodium pentobarbital at 1, 2, 3, 4 and 8 weeks postop, respectively. The CSDs sites were removed with a small amount of surrounding bone. Following observation with

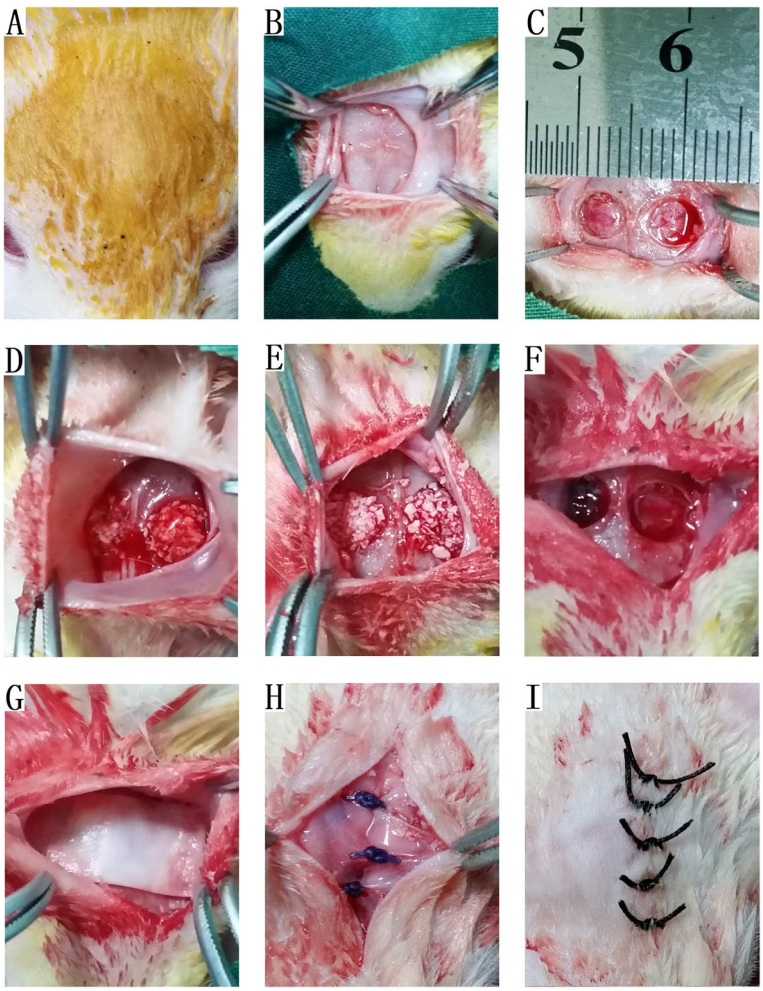

Fig. 1 Surgical procedures. **A** SD rats were anesthetized and the skull was disinfected. **B** An incision was made and the periosteum was elevated and reflected. **C** Two symmetrical round full-thickness calvarial CSDs (5 mm in diameter) were created. **D** CSDs were grafted with HA-DBBM compound. **E** CSDs were grafted with DBBM particles only. **F** CSDs with no graft. **G** A bioresorbable collagen membrane was used to cover the surgical site. **H** The periosteum was sutured. **I** The skin was sutured

a digital camera (Nikon, Tokyo, Japan), the samples were immediately fixed in 4% buffered formalin for 24 h.

Micro-CT scanning

Samples harvested 8 weeks postop were placed on the base of a high-resolution Micro-CT scanner (Inveon, Siemens, Germany). The calvarial CSDs were set as the region of interest (ROI). The scanning parameters were as follows: 80 kV, 500 μA with a 2500 ms exposure time. The resolution was set at 19.64 μm and the rotation step of 0.67. The samples were reconstructed three-dimensionally using software Mimics 10.01 (Materialise, Leuven, Belgium). The bone volume/tissue volume (BV/TV), trabecular number (Tb.N), trabecular thickness (Tb.Th), trabecular space (Tb.Sp) and trabecular pattern factor (Tb.Pf) of the ROIs in each sample were analyzed.

Hematoxylin and eosin (HE) staining

Samples harvested 2 and 4 weeks postop and those after Micro-CT scanning (8 weeks postop) were decalcified in EDTA solution (Merck, Darmstadt, Germany) for 30 days. The specimens were trimmed using a precision saw and dehydrated in graded alcohol. The CSDs were identified visually, followed by cutting into halves along the center of two defects. The samples were embedded in paraffin. Sections were cut into 4 μm thickness and stained with HE. HE stained sections were observed under a light microscope (Leica Microsystems, Wetzlar, Germany) connected to a digital camera. The percentage of newly formed bone area within the defect area was determined by a single blinded, calibrated examiner using imaging software (ImageJ, National Institutes of Health, Bethesda, USA).

Statistical analysis

All experiments were repeated at least three times. All data were expressed as mean ± standard deviation. Analyses were performed using SPSS 16.0 (SPSS Inc., Chicago, USA). One-way analysis of variance (ANOVA) followed by Tukey's post hoc test were performed for multiple comparisons. Differences were considered significant if $P < 0.05$.

Results

Clinical observation of rat calvarial CSDs

There was no complication during surgery. All rats survived after surgery. One rat had wound dehiscence one day postop. After intraperitoneal reinjection of 1% pentobarbital sodium and re-suturing, the rat recovered well. No signs of clinical infection or necrosis of the wound were observed at any test time point. The clinical observation of rat calvarial CSDs 1, 2, 3, 4 and 8 weeks postop was shown in Fig. 2.

One week postop, there was abundant connective tissue in CSDs area of the HA-DBBM compound grafting group and DBBM particles only grafting group. The DBBM particles were embedded within the fiber-rich connective tissue. In the no graft group, only little connective tissue was observed in the rim of the CSDs area, while the remainder of the CSDs area was hollow. Two weeks postop, there was much denser and more connective tissue in CSDs area in the HA-DBBM compound grafting group and DBBM particles only grafting group. In the no graft group, the hollowed CSDs area was reduced. Additionally, there was much more connective tissue, which was mainly distributed along the rim of the CSDs area. With time prolonged and the wound healing processed, there was increasingly much more new bone tissue formed in CSDs area of the HA-DBBM compound grafting group and DBBM particles only grafting group. There was much more connective tissue in CSDs area of the no graft group. New bone tissue formed later and less in the no graft group than in the other two groups.

Histology and histomorphometry of rat calvarial CSDs

Defect sites were harvested 2, 4, and 8 weeks after calvarial implantation to evaluate bone regeneration. The histologic sections are shown in Figs. 3 and 4. The results of the histomorphometric analysis are shown in Fig. 5. As expected, HA-DBBM compound grafting group exhibited the highest bone-healing efficacy.

In the HA-DBBM compound grafting group, a large amount of connective tissue, little new bone tissue and few blood vessels were observed in the rim of the CSDs area at low-magnification 2 weeks postop. The DBBM particles were surrounded by fiber-rich connective tissue (Fig. 3 A2). The new bone tissue was immature at high-magnification (Fig. 4 A2). Four weeks postop, there was much more new bone tissue and blood vessels. Many mononuclear cells and a few giant cells were observable on the surfaces of DBBM particles at this time point (Figs. 3 A4 and 4 A4). Eight weeks postop, there was an increasing amount of mature new bone tissue. The intergranular connective tissue and the DBBM particles exhibited a fiber-and vessel-rich composition. At this time, there was space around the DBBM particles, and the majority of the cells were mononuclear, while a minority of cells were multinuclear on the surfaces of DBBM particles (Figs. 3 A8 and 4 A8).

In the DBBM particles only grafting group, little new bone tissue and much more fiber-rich connective tissue could be noted in the rim of the CSDs area at low-magnification 2 weeks postop. The DBBM particles were embedded in fiber-rich connective tissue (Fig. 3 B2). Four weeks postop, more new bone tissue and blood vessels had formed (Figs. 3 B4 and 4 B4). The new bone tissue

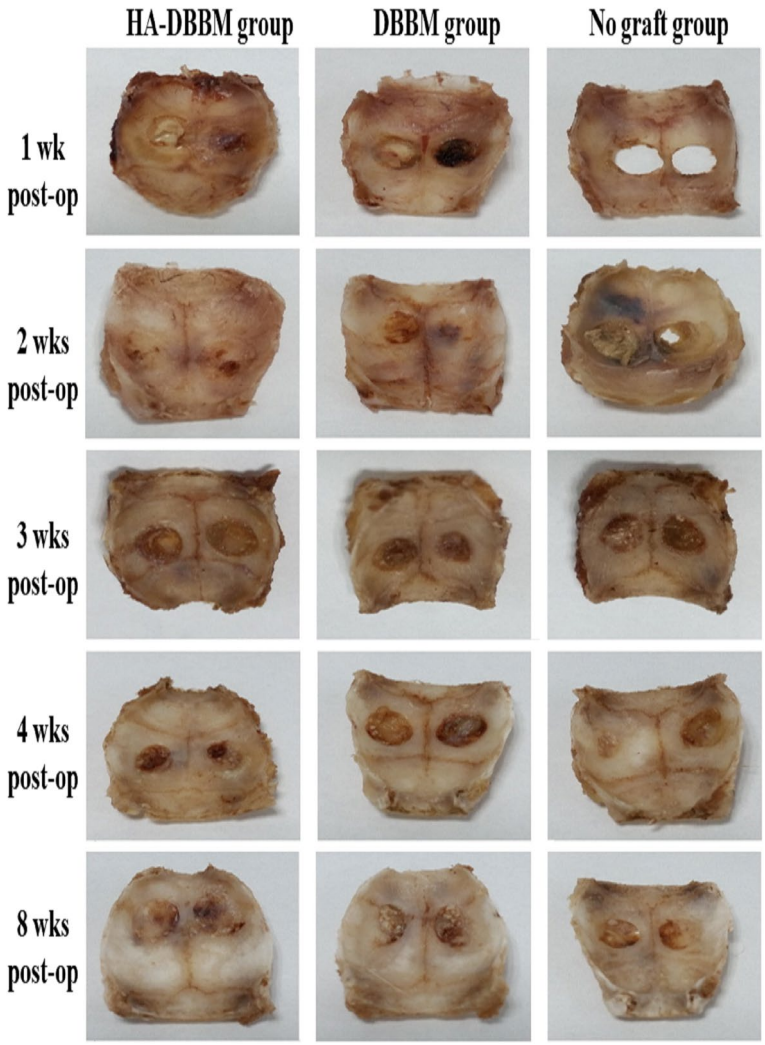

Fig. 2 Clinical observation of rat calvarial CSDs at 1, 2, 3, 4 and 8 weeks postop

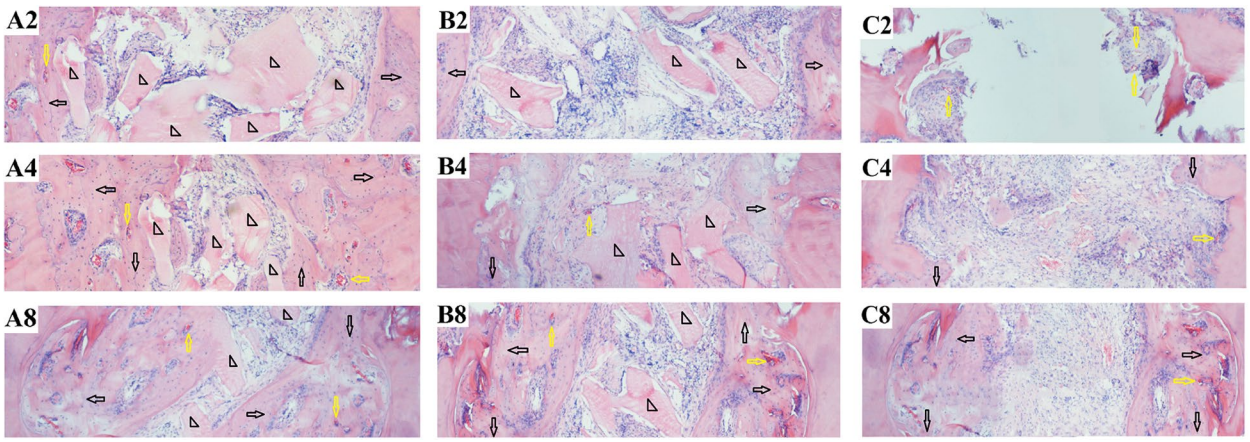

Fig. 3 HE staining images of rat calvarial CSDs. **A**: HA-DBBM compound grafting group. **B**: DBBM particles only grafting group. **C**: no graft group. 2, 4 and 8 refer to 2, 4 and 8 weeks postop, respectively. Black arrow: new bone; black triangle: DBBM particles; yellow arrow: blood vessel. Magnification, × 20)

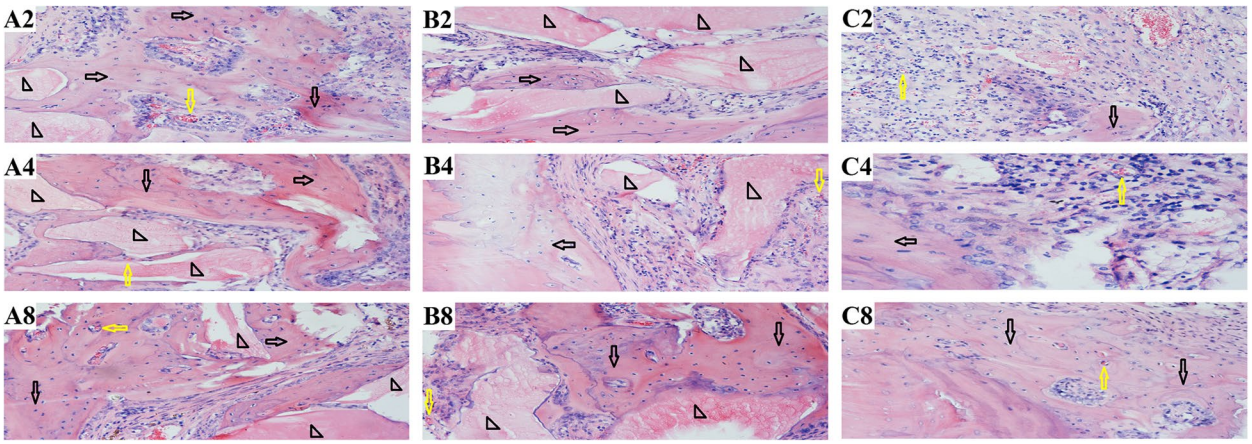

Fig. 4 HE staining images of rat calvarial CSDs. **A**: HA-DBBM compound grafting group. **B**: DBBM particles only grafting group. **C**: no graft group. 2, 4 and 8 refer to 2, 4 and 8 weeks postop, respectively. Black arrow: new bone; black triangle: DBBM particles; yellow arrow: blood vessel. Magnification, × 200)

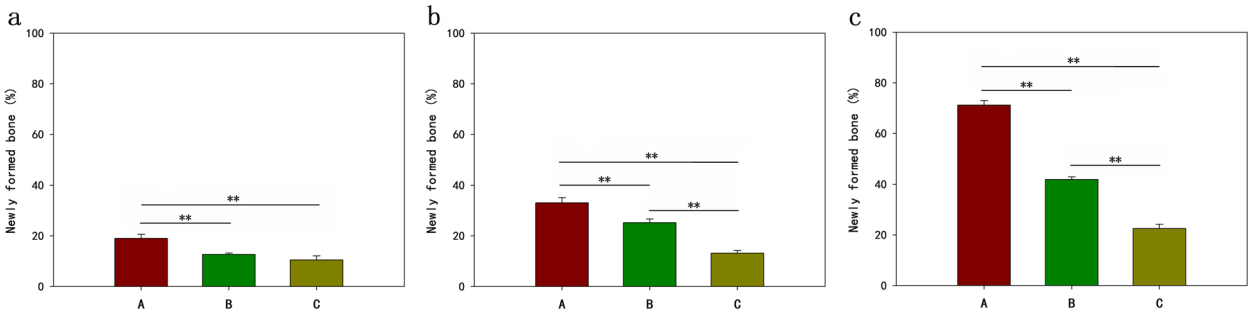

Fig. 5 The percentage of newly formed bone in rat calvarial CSDs 2 weeks (**a**), 4 weeks (**b**) and 8 weeks (**c**) postop. **A**: HA-DBBM compound grafting group. **B**: DBBM particles only grafting group. **C**: no graft group

was markedly more and more mature at 8 weeks postop (Figs. 3 B8 and 4 B8).

In the no graft group, little connective tissue was observed in the rim of the CSDs area at low-magnification 2 weeks postop. The inner part of the CSDs area was hollow (Figs. 3 C2 and 4 C2). Four weeks postop, little new bone tissue could be found in the rim of the CSDs area, with the remaining part of the CSDs area filled with fiber-rich connective tissue (Figs. 3 C4 and 4 C4). Eight weeks postop, the amount of new bone tissue increased, however, new bone tissue still existed in the rim of the CSDs area. The inner part of the CSDs area was filled with fiber-rich connective tissue (Figs. 3 C8 and 4 C8).

At 2 weeks after the operation, the percentage of newly formed bone was significantly greater in the HA-DBBM compound grafting group (18.99 ± 1.64) than in the other two groups (Fig. 5a, $P < 0.01$, respectively). However, there was no significant difference in the percentage of newly formed bone between the DBBM particles only grafting group (12.64 ± 0.56) and the no graft group (10.50 ± 1.57) (Fig. 5a, $P = 0.12$). Four weeks postop, the percentage of newly formed bone was significantly greater in the HA-DBBM compound grafting group (33.08 ± 2.00) than in the DBBM particles only grafting group (25.20 ± 1.45) and the no graft group (13.15 ± 1.05) (Fig. 5b, $P < 0.01$, respectively). The differences were significant between each two groups. At 8 weeks postop, the percentage of newly formed bone was significantly greater in the HA-DBBM compound grafting group (71.19 ± 1.81) than the DBBM particles only grafting group (41.89 ± 1.07) and the no graft group (22.52 ± 1.71) (Fig. 5c, $P < 0.01$, respectively). The differences were significant between each two groups.

3D reconstruction images of the rat calvarial CSDs

Micro-CT scanning was performed for rats sacrificed 8 weeks postop. The 3D reconstructed images after Micro-CT scanning were shown in Fig. 6. The new bone tissue was obvious and continuous, and filled the CSDs area in the HA-DBBM compound grafting group. The DBBM particles were surrounded by abundant new bone tissue (Fig. 6A). In the DBBM particles only grafting group,

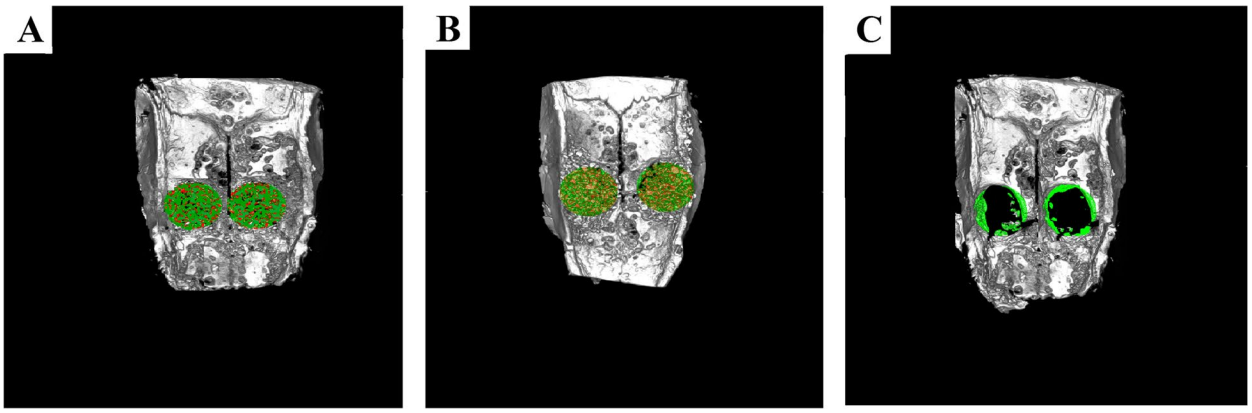

Fig. 6 3D reconstruction images after Micro-CT scanning of rat calvarial CSDs 8 weeks postop. **A**: HA-DBBM compound grafting group. **B**: DBBM particles only grafting group. **C**: no graft group. The red and green colours indicate the DBBM particles and the new bone tissue, respectively

new bone tissue was found in the whole CSDs area. However, the newly formed bone tissue was less and less continuous than that in the HA-DBBM compound grafting group. New bone tissue and the DBBM particles were closely connected (Fig. 6B). In the no graft group, less new bone tissue formed in the rim of the CSDs area than the other two groups. In addition, the new bone tissue was less continuous than the other two groups (Fig. 6C).

Bone parameter analysis of rat calvarial CSDs

After Micro-CT scanning, bone parameter analysis of rat calvarial CSDs was carried out. Figure 7 shows the statistical results. The BV/TV ratios for the HA-DBBM compound grafting group, DBBM particles only grafting group and the no graft group were 85.22 ± 3.66%, 52.58 ± 2.97% and 21.90 ± 2.64%, respectively. There were significant differences among the three groups ($P < 0.01$, respectively). Moreover, there was significant difference between each two groups (Fig. 7a, $P < 0.01$, respectively). The BV/TV ratio of the HA-DBBM compound grafting group was 1.62 and 3.89 times greater than those of the DBBM particles only grafting group and the no graft group, respectively. A similar trend was also found for the Tb.N. The Tb.N values for the three groups were 8.98 ± 0.10, 5.11 ± 0.18 and 0.93 ± 0.07, respectively. There were significant differences among the three groups and

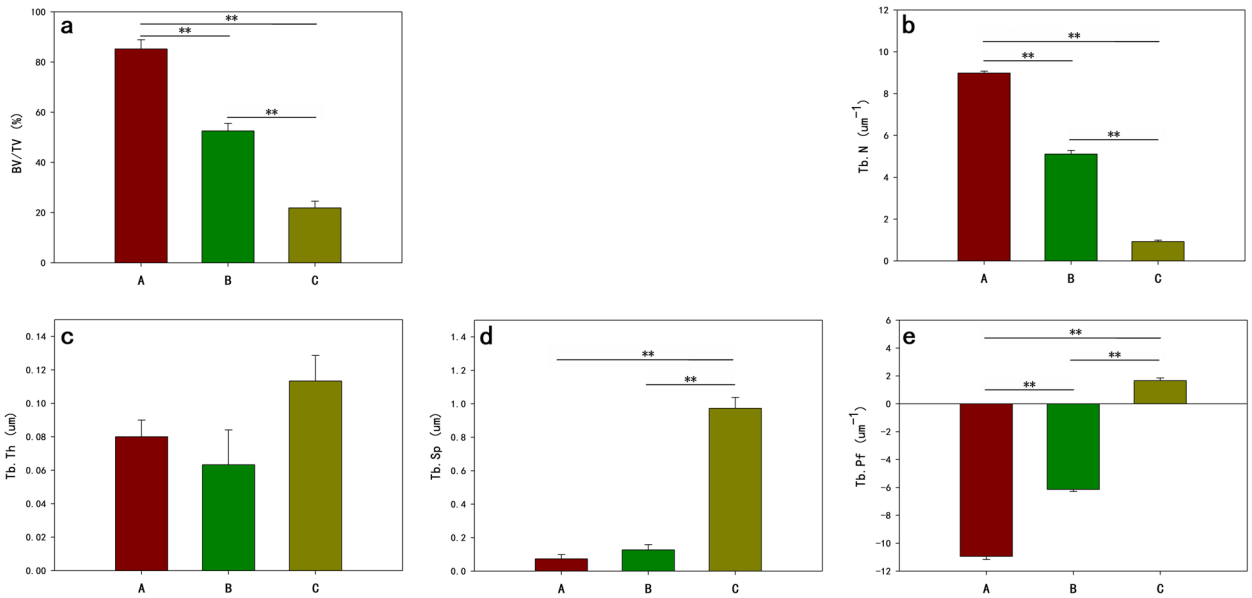

Fig. 7 Statistical analysis of the bone parameters of rat calvarial CSDs 8 weeks postop. **A**: HA-DBBM compound grafting group. **B**: DBBM particles only grafting group. **C**: no graft group. $^{**}P < 0.01$

between each two groups (Fig. 7b, $P < 0.01$, respectively). The Tb.N of the HA-DBBM compound grafting group was 1.76 and 9.66 times greater than those of the DBBM particles only grafting group and the no graft group, respectively.

For Tb.Th there was no significant difference among the three groups, or between each two groups (Fig. 7c, $P > 0.05$, respectively). With respect to the Tb.Sp, there were significant differences among the three groups ($P < 0.01$, respectively). There were significant differences between the HA-DBBM compound grafting group and the no graft group, DBBM particles only grafting group and the no graft group, respectively ($P < 0.01$, respectively). However, there was no significant difference between the HA-DBBM compound grafting group and DBBM particles only grafting group (Fig. 7d, $P > 0.05$). The Tb.Sp of the no graft group was significantly greater than that of the other two groups ($P < 0.01$, respectively).

For Tb.Pf there were significant differences among the three groups and between each two groups (Fig. 7e, $P < 0.01$, respectively). The Tb.Pf of the HA-DBBM compound grafting group was significantly lower than that of the other two groups ($P < 0.01$, respectively).

Discussion

Our study demonstrated that the combination of high-MW HA with bone substitute particles stimulates more new bone tissue, increases trabecular number, improves trabecular connectivity, and increases new bone formation within CSDs in rat calvaria. Thus, the null hypothesis was rejected. The results could provide scientific evidence for further optimizing the properties of bone substitute particles.

GBR has become a fundamental concept of bone augmentation and is widely used in dental implant therapy, moreover, the restoration of periodontal defects [39], and promising bone regeneration results have been obtained [40]. As is known to all that different materials used in GBR can result in different capacity of bone regeneration. Various bone substitute and techniques have been developed and provided for bone defects repairing and bone tissue regeneration. To thoroughly evaluate the efficacy and applicability of these materials and techniques, preclinical experimental models are indispensable. Among these, the animal calvarial CSDs model stands out due to several distinct advantages, such as convenience for accessibility, standardization of defect dimension, and the support of bone substitute by dura and skin [41]. Moreover, it makes the results more relevant than those obtained from heterotopic models. Therefore, calvarial CSDs model is extensively utilized to assess the effect of bone substitute on defect healing [42].

Many species have been employed as calvarial CSDs model, including rats [43, 44], rabbits [45, 46], dogs, sheep, goats and pigs [47–50]. Rat calvaria CSDs model has become one of most commonly used experimental models for evaluating the new bone formation capacity of bone substitute, due to its high cost-effectiveness, easy housing and feeding, high reproducibility, and realization of standard experimental conditions in genetically similar individuals [51, 52]. Therefore, in our study, we utilized rat and established rat calvaria CSDs.

Angiogenesis is a critical early event in the tissue repair process, typically preceding osteogenesis. The newly formed blood vessels provide nutritional support and steady transportation of osteoblast and osteoclast precursors to the remodeling bone [53]. In our study, at 2 weeks postop, angiogenesis was found in the connective tissue, which embedded DBBM particles in the implantation site in HA-DBBM compound grafting group. This could be attributed to the angiogenesis-promoting properties of high-MW HA.

An important aspect to evaluate the new bone formation capacity of bone substitutes is their ability to remain stable within the implantation bed, and maintain the space for tissue regeneration [54]. Position change and degradation of bone substitutes in implantation bed could destroy tissue repair, because the bone substitutes has not yet been replaced by the newly formed bone tissue [55, 56]. Smaller fragments of DBBM particles might play a role in cellular responses and vascularization, which is indispensable for the successful integration of DBBM particles and surrounding tissues.

In the histopathological section of HA-DBBM compound grafting group and DBBM particles only grafting group, we found some space and many monocytes around DBBM particles. These findings were consistent with the results reported by Tamimi et al. and Sartori et al. [57, 58]. On the one hand, the space might result from the absorption of the DBBM particles. The slow absorption of DBBM particles could not only maintain the implantation space, but also be in favor of vascularization and the ingrowth of new bone tissue. This idea was shared with Piattelli et al., who utilized DBBM particles in human sinus augmentation. They found that DBBM particles was surrounded by abundant newly formed lamellar bone in all 20 cases 4 years post grafting [59]. Notably, the inner core of DBBM particles remained intact [59]. Compared with other bone substitute, DBBM particles tended to promote more early bone formation, at the same time, undergoing a very slow absorption [60]. However, some researchers indicated that because of the non-resorbability of DBBM particles, regeneration of bone defects in beagle dogs could be achieved [61]. Schlegel et al. claimed that the volume reduction of

DBBM particles could be explained by shrinkage rather than resorption [61]. On the other hand, we assume that the space might arise from the biodegradation of high-MW HA, which requires further investigation. Additionally, the specific nature and the action mode of the monocytes warrant deeper exploration.

Within the study period, we found that the HA-DBBM compound grafting group exhibited a higher quantity of new bone tissue and an earlier onset of bone formation compared to the other two groups. Quantitative analysis of bone parameters indicated that the BV/TV and Tb.N of the HA-DBBM compound grafting group were significantly greater than those of the other two groups. These results indicated that the HA-DBBM compound was particularly effective in promoting both the quantity of new bone formation and the density of trabecular structures, which was in consistent with the 3D reconstruction images. The Tb.Pf was significantly lower in the HA-DBBM compound grafting group, indicative of enhanced connectivity between the trabeculae. Conversely, the Tb.Sp was significantly greater in the no graft group than in the other two groups, highlighting the pronounced impact of the HA-DBBM compound on reducing the intertrabecular spaces and promoting a denser bone matrix. The findings of our study were consistent with the results reported by Matheus et al. and Kim et al. [62, 63] However, Agrali et al. [64] reported that the HA matrix, used alone or in combination with resorbable collagen membrane and bovine-derived xenograft, did not contribute significantly to bone regeneration in rat calvarial bone defects. Diker et al. [65] demonstrated that HA alone did not adequately enhance bone regeneration in rat CSDs. Moreover, the addition of HA to hydroxyapatite/beta-tricalcium phosphate graft material did not result in improved regeneration compared with that of the graft material alone [65]. The observed discrepancies of these studies may be attributed to the use of HA with relatively lower MW.

It is widely acknowledged that autologous bone is the gold standard for bone grafting. However, the increase in new bone formation resulting from the combination of high-MW HA and a commercially available bone substitute encouraged researchers to evaluate the cost-effectiveness of the HA-DBBM compound and the morbidity of harvesting autogenous bone. In addition, high-MW HAs are viscoelastic and improves the handling ability of bone substitute particles as osteoconductive scaffolds.

Admittedly, the study has some limitations. Firstly, the mechanism by which high-MW HA and its degradation in combination with the HA-DBBM compound promote new bone formation in rat calvaria CSDs necessitates further in-depth investigation. Secondly, the effect of HA on new bone formation depends on HA concentration, MW, and HA/bone substitute ratio. It would be interesting to investigate the influence of these variables on new bone formation in future study.

Conclusions

The formation of new bone is the purpose of bone regeneration and determines whether the biomaterial was successful for that purpose. Notwithstanding its limitations, this study demonstrated that the combination of high-MW HA with bone substitute particles stimulated more new bone tissue, increased trabecular number, improved trabecular connectivity, and increased new bone formation within CSDs in rat calvaria when compared to using bone substitute particles alone or no graft. This advancement could potentially offer a more effective strategy for bone regeneration.

Abbreviations

MW	Molecular weight
HA	Hyaluronic acid
DBBM	Deproteinized bovine bone mineral
CSD	Calvarial critical size defect
SD rats	Sprague–Dawley rats
ROI	Region of interest
BV/TV	Bone volume/tissue volume
Tb.N	Trabecular number
Tb.Th	Trabecular thickness
Tb.Sp	Trabecular space
Tb.Pf	Trabecular pattern factor
HE	Hematoxylin and eosin

Acknowledgements

Not applicable.

Authors' contributions

NB Zhao conducted the experimental procedures, collected and analyzed the data, drafted the manuscript and secured the funding for the study. LQ, and YL conducted the animal experiments and critically revised the manuscript. MZ analyzed the data and critically revised the manuscript. DH Li conceptualized and designed the study, critically revised the manuscript and approved the final version of the article. All authors reviewed and approved the final manuscript.

Funding

The study was funded by the National Natural Science Foundation of China (No. 82001085) and the New Technology and Project at College of Stomatology, Xi'an Jiaotong University (No. xjkqxjs2021-14).

Availability of data and materials

All essential data is presented in the manuscript. The datasets used and/or analysed during the current study are available from the corresponding author on reasonable request.

Declarations

Ethics approval and consent to participate

All the experimental procedures were approved by the Laboratory Animal Care & Welfare Committee, School of Stomatology, Fourth Military Medical University.

Consent for publication

Not applicable.

Competing interests

The authors declare no competing interests.

Received: 20 April 2024 Accepted: 29 July 2024
Published online: 24 August 2024

References

1. Adell R, Lekholm U, Rockler B, Brånemark P-I. A 15-year study of osseointegrated implants in the treatment of the edentulous jaw. Int J Oral Surg. 1981;10(6):387–416.
2. Karoussis IK, Kotsovilis S, Fourmousis I. A comprehensive and critical review of dental implant prognosis in periodontally compromised partially edentulous patients. Clin Oral Implant Res. 2007;18(6):669–79.
3. Lang NP, Pjetursson BE, Tan K, Brägger U, Egger M, Zwahlen M. A systematic review of the survival and complication rates of fixed partial dentures (FPDs) after an observation period of at least 5 years: II. Combined tooth–implant-supported FPDs. Clin Oral Implants Res. 2004;15(6):643–53.
4. Revilla-León M, Yilmaz B, Kois JC, Att W. Prevention of peri-implant disease in edentulous patients with fixed implant rehabilitations. Clin Implant Dent Relat Res. 2023;25(4):743–51.
5. Roccuzzo A, Imber JC, Lempert J, Hosseini M, Jensen SS. Narrow diameter implants to replace congenital missing maxillary lateral incisors: A 1-year prospective, controlled, clinical study. Clin Oral Implant Res. 2022;33(8):844–57.
6. Clark D, Levin L. In the dental implant era, why do we still bother saving teeth? J Endod. 2019;45(12):S57–65.
7. Decker AM, Kapila YL, Wang HL. The psychobiological links between chronic stress-related diseases, periodontal/peri-implant diseases, and wound healing. Periodontology 2000. 2021;87(1):94–106.
8. Zhao L, Hu W, Liu Y, Chung KH. Evaluation of implant placement following ridge preservation in periodontally compromised molar extraction sockets: Three-year results of a prospective cohort study. Clin Oral Implant Res. 2022;33(7):735–44.
9. Benic GI, Hämmerle CH. Horizontal bone augmentation by means of guided bone regeneration. Periodontol 2000. 2014;66(1):13–40.
10. Kungvarnchaikul I, Subbalekha K, Sindhavajiva PR, Suwanwela J. Deproteinized bovine bone and freeze-dried bone allograft in sinus floor augmentation. Clin Implant Dent Relat Res. 2023;25(2):343–51.
11. Chen X, Wang H, Wang Y, Shi Y, Wang Z. Enhanced osteogenesis by addition of cancellous bone chips at xenogenic bone augmentation: In vitro and in vivo experiments. Clin Oral Implant Res. 2023;34(1):42–55.
12. Yu H, Niu L, Qiu L. Histologic and Clinical Evaluation of Ridge Augmentation of Extraction Sockets with Severe Bone Defects: A Clinical Prospective Study. Int J Oral Maxillofac Implans. 2022;37(4):778–83.
13. Shen X, Yang S, Xu Y, Qi W, He F. Marginal bone loss of tissue-or bone-level implants after simultaneous guided bone regeneration in the posterior mandibular region: A retrospective cohort study. Clin Implant Dent Relat Res. 2023;25(1):68–76.
14. Naujokat H, Açil Y, Harder S, Lipp M, Böhrnsen F, Wiltfang J. Osseointegration of dental implants in ectopic engineered bone in three different scaffold materials. Int J Oral Maxillofac Surg. 2020;49(1):135–42.
15. Caubet J, Ramis JM, Ramos-Murguialday M, Morey MÁ, Monjo M. Gene expression and morphometric parameters of human bone biopsies after maxillary sinus floor elevation with autologous bone combined with Bio-Oss® or BoneCeramic®. Clin Oral Implant Res. 2015;26(6):727–35.
16. Jensen T, Schou S, Stavropoulos A, Terheyden H, Holmstrup P. Maxillary sinus floor augmentation with Bio-Oss or Bio-Oss mixed with autogenous bone as graft: a systematic review. Clin Oral Implant Res. 2012;23(3):263–73.
17. de Sousa CA, Lemos CAA, Santiago-Júnior JF, Faverani LP, Pellizzer EP. Bone augmentation using autogenous bone versus biomaterial in the posterior region of atrophic mandibles: A systematic review and meta-analysis. J Dent. 2018;76:1–8.
18. McAllister BS, Haghighat K. Bone augmentation techniques. J Periodontol. 2007;78(3):377–96.
19. Huh J-B, Yang J-J, Choi K-H, Bae JH, Lee J-Y, Kim S-E, Shin S-W. Effect of rhBMP-2 immobilized anorganic bovine bone matrix on bone regeneration. Int J Mol Sci. 2015;16(7):16034–52.
20. Arias-Gallo J, Chamorro-Pons M, Avendaño C, Giménez-Gallego G. Influence of acidic fibroblast growth factor on bone regeneration in experimental cranial defects using spongostan and Bio-Oss as protein carriers. J Craniofac Surg. 2013;24(5):1507–14.
21. Kuo P-J, Yen H-J, Lin C-Y, Lai H-Y, Chen C-H, Wang S-H, et al. Estimation of the effect of accelerating new bone formation of high and low molecular weight hyaluronic acid hybrid: An animal study. Polymers. 2021;13(11):1708.
22. Park K. Injectable hyaluronic acid hydrogel for bone augmentation. J Control Release. 2011;2(152):207.
23. Wang H-L, Boyapati L. "PASS" principles for predictable bone regeneration. Implant Dent. 2006;15(1):8–17.
24. Abatangelo G, Vindigni V, Avruscio G, Pandis L, Brun P. Hyaluronic acid: redefining its role Cells. 2020;9(7):1743.
25. Teng B, Zhang S, Pan J, Zeng Z, Chen Y, Hei Y, et al. A chondrogenesis induction system based on a functionalized hyaluronic acid hydrogel sequentially promoting hMSC proliferation, condensation, differentiation, and matrix deposition. Acta Biomater. 2021;122:145–59.
26. Zhao N, Wu Z, Qin L, Guo Z, Li D. Characteristics and tissue regeneration properties of gingiva-derived mesenchymal stem cells. Crit Rev Eukaryot Gene Expr. 2015;25(2):135–44.
27. Dong Y, Cui M, Qu J, Wang X, Kwon SH, Barrera J, et al. Conformable hyaluronic acid hydrogel delivers adipose-derived stem cells and promotes regeneration of burn injury. Acta Biomater. 2020;108:56–66.
28. Vaca-González JJ, Clara-Trujillo S, Guillot-Ferriols M, Ródenas-Rochina J, Sanchis MJ, Ribelles JLG, et al. Effect of electrical stimulation on chondrogenic differentiation of mesenchymal stem cells cultured in hyaluronic acid–Gelatin injectable hydrogels. Bioelectrochemistry. 2020;134: 107536.
29. Casale M, Moffa A, Vella P, Sabatino L, Capuano F, Salvinelli B, et al. Hyaluronic acid: Perspectives in dentistry. A systematic review. Int J Immunopathol Pharmacol. 2016;29(4):572–82.
30. Boeckel DG, Shinkai RSA, Grossi ML, Teixeira ER. In vitro evaluation of cytotoxicity of hyaluronic acid as an extracellular matrix on OFCOL II cells by the MTT assay. Oral Surg Oral Med Oral Pathol Oral Radiol. 2014;117(6):e423–8.
31. Asparuhova MB, Chappuis V, Stähli A, Buser D, Sculean A. Role of hyaluronan in regulating self-renewal and osteogenic differentiation of mesenchymal stromal cells and pre-osteoblasts. Clin Oral Invest. 2020;24:3923–37.
32. Amann E, Wolff P, Breel E, Van Griensven M, Balmayor ER. Hyaluronic acid facilitates chondrogenesis and matrix deposition of human adipose derived mesenchymal stem cells and human chondrocytes co-cultures. Acta Biomater. 2017;52:130–44.
33. Sasaki T, Watanabe C. Stimulation of osteoinduction in bone wound healing by high-molecular hyaluronic acid. Bone. 1995;16(1):9–15.
34. Kim SE, Lee JY, Shim K-S, Lee S, Min K, Bae J-H, et al. Attenuation of inflammation and cartilage degradation by sulfasalazine-containing hyaluronic acid on osteoarthritis rat model. Int J Biol Macromol. 2018;114:341–8.
35. Raines AL, Sunwoo M, Gertzman AA, Thacker K, Guldberg RE, Schwartz Z, Boyan BD. Hyaluronic acid stimulates neovascularization during the regeneration of bone marrow after ablation. J Biomed Mater Res, Part A. 2011;96(3):575–83.
36. Romanò C, Vecchi ED, Bortolin M, Morelli I, Drago L. Hyaluronic acid and its composites as a local antimicrobial/antiadhesive barrier. Journal of bone and joint infection. 2017;2(1):63–72.
37. Zhao N, Wang X, Qin L, Guo Z, Li D. Effect of molecular weight and concentration of hyaluronan on cell proliferation and osteogenic differentiation in vitro. Biochem Biophys Res Commun. 2015;465(3):569–74.
38. Kim JJ, Song HY, Ben Amara H, Kyung-Rim K, Koo KT. Hyaluronic acid improves bone formation in extraction sockets with chronic pathology: a pilot study in dogs. J Periodontol. 2016;87(7):790–5.
39. de Brito BB, Mendes Brazão MA, de Campos MLG, Casati MZ, Sallum EA, Sallum AW. Association of hyaluronic acid with a collagen scaffold may improve bone healing in critical-size bone defects. Clin Oral Implant Res. 2012;23(8):938–42.
40. Elgali I, Omar O, Dahlin C, Thomsen P. Guided bone regeneration: materials and biological mechanisms revisited. Eur J Oral Sci. 2017;125(5):315–37.
41. Gomes P, Fernandes M. Rodent models in bone-related research: the relevance of calvarial defects in the assessment of bone regeneration strategies. Lab Anim. 2011;45(1):14–24.
42. Mariano R, Messora M, de Morais A, Nagata M, Furlaneto F, Avelino C, et al. Bone healing in critical-size defects treated with platelet-rich plasma: a histologic and histometric study in the calvaria of diabetic rat. Oral Surgery, Oral Medicine, Oral Pathology, Oral Radiology, and Endodontology. 2010;109(1):72–8.

43. Lohmann P, Willuweit A, Neffe A, Geisler S, Gebauer T, Beer S, et al. Bone regeneration induced by a 3D architectured hydrogel in a rat critical-size calvarial defect. Biomaterials. 2017;113:158–69.
44. Mokbel N, Bou Serhal C, Matni G, Naaman N. Healing patterns of critical size bony defects in rat following bone graft. Oral Maxillofac Surg. 2008;12:73–8.
45. Pelegrine AA, Aloise AC, Zimmermann A, de Oliveira RME, Ferreira LM. Repair of critical-size bone defects using bone marrow stromal cells: a histomorphometric study in rabbit calvaria. Part I: Use of fresh bone marrow or bone marrow mononuclear fraction. Clin Oral Implants Res. 2014;25(5):567–72.
46. Grossi-Oliveira G, Faverani LP, Mendes BC, Braga Polo TO, Batista Mendes GC, Lima VNd, et al. Comparative evaluation of bone repair with four different bone substitutes in critical size defects. Int J Biomater. 2020;2020:5182845.
47. Niemeyer P, Fechner K, Milz S, Richter W, Suedkamp NP, Mehlhorn AT, et al. Comparison of mesenchymal stem cells from bone marrow and adipose tissue for bone regeneration in a critical size defect of the sheep tibia and the influence of platelet-rich plasma. Biomaterials. 2010;31(13):3572–9.
48. Huh J-Y, Choi B-H, Kim B-Y, Lee S-H, Zhu S-J, Jung J-H. Critical size defect in the canine mandible. Oral Surg Oral Med Oral Pathol Oral Radiol Endod. 2005;100(3):296–301.
49. Sun Z, Kennedy KS, Tee BC, Damron JB, Allen MJ. Establishing a critical-size mandibular defect model in growing pigs: characterization of spontaneous healing. J Oral Maxillofac Surg. 2014;72(9):1852–68.
50. Chu W, Gan Y, Zhuang Y, Wang X, Zhao J, Tang T, Dai K. Mesenchymal stem cells and porous β-tricalcium phosphate composites prepared through stem cell screen-enrich-combine (– biomaterials) circulating system for the repair of critical size bone defects in goat tibia. Stem Cell Res Ther. 2018;9(1):1–12.
51. Huang EE, Zhang N, Shen H, Li X, Maruyama M, Utsunomiya T, et al. Novel techniques and future perspective for investigating critical-size bone defects. Bioengineering. 2022;9(4):171.
52. Vajgel A, Mardas N, Farias BC, Petrie A, Cimões R, Donos N. A systematic review on the critical size defect model. Clin Oral Implant Res. 2014;25(8):879–93.
53. Saran U, Piperni SG, Chatterjee S. Role of angiogenesis in bone repair. Arch Biochem Biophys. 2014;561:109–17.
54. Tapety FI, Amizuka N, Uoshima K, Nomura S, Maeda T. A histological evaluation of the involvement of Bio-Oss® in osteoblastic differentiation and matrix synthesis. Clin Oral Implant Res. 2004;15(3):315–24.
55. Ghanaati S, Barbeck M, Orth C, Willershausen I, Thimm BW, Hoffmann C, et al. Influence of β-tricalcium phosphate granule size and morphology on tissue reaction in vivo. Acta Biomater. 2010;6(12):4476–87.
56. Accorsi-Mendonça T, Conz MB, Barros TC, Sena LÁd, Soares GdA, Granjeiro JM. Physicochemical characterization of two deproteinized bovine xenografts. Braz oral Res. 2008;22:5–10.
57. Tamimi FM, Torres J, Tresguerres I, Clemente C, López-Cabarcos E, Blanco LJ. Bone augmentation in rabbit calvariae: comparative study between Bio-Oss® and a novel β-TCP/DCPD granulate. J Clin Periodontol. 2006;33(12):922–8.
58. Sartori S, Silvestri M, Forni F, Icaro Cornaglia A, Tesei P, Cattaneo V. Ten-year follow-up in a maxillary sinus augmentation using anorganic bovine bone (Bio-Oss). A case report with histomorphometric evaluation. Clin Oral Implants Res. 2003;14(3):369–72.
59. Piattelli M, Favero GA, Scarano A, Orsini G, Piattelli A. Bone reactions to anorganic bovine bone (Bio-Oss) used in sinus augmentation procedures: a histologic long-term report of 20 cases in humans. Int J Oral Maxillofac Implants. 1999;14(6):835–40.
60. Klinge B, Alberius P, Isaksson S, Jönsson J. Osseous response to implanted natural bone mineral and synthetic hydroxylapatite ceramic in the repair of experimental skull bone defects. J Oral Maxillofac Surg. 1992;50(3):241–9.
61. Schlegel KA, Fichtner G, Schultze-Mosgau S, Wiltfang J. Histologic findings in sinus augmentation with autogenous bone chips versus a bovine bone substitute. Int J Oral Maxillofac Implants. 2003;18(1):53–8.
62. Matheus HR, Ervolino E, Gusman DJR, Alves BES, Fiorin LG, Pereira PA, de Almeida JM. Association of hyaluronic acid with a deproteinized bovine graft improves bone repair and increases bone formation in critical-size bone defects. J Periodontol. 2021;92(11):1646–58.
63. Kim JJ, Ben Amara H, Park Jc, Kim S, Kim TI, Seol YJ, et al. Biomodification of compromised extraction sockets using hyaluronic acid and rhBMP-2: an experimental study in dogs. J Periodontol. 2019;90(4):416–24.
64. Agrali OB, Yildirim S, Ozener HO, Köse KN, Ozbeyli D, Soluk-Tekkesin M, Kuru L. Evaluation of the effectiveness of esterified hyaluronic acid fibers on bone regeneration in rat calvarial defects. BioMed Res Int. 2018;2018:3874131.
65. Diker N, Gulsever S, Koroglu T, Akcay EY, Oguz Y. Effects of hyaluronic acid and hydroxyapatite/beta-tricalcium phosphate in combination on bone regeneration of a critical-size defect in an experimental model. J Craniofac Surg. 2018;29(4):1087–93.

Publisher's Note